

Flow Characteristics of Plane Wall Jet with Side Walls on Both Sides*

Shigeki IMAO**, Satoshi KIKUCHI**, Yasuaki KOZATO** and Takayasu HAYASHI***

Flow characteristics of a two-dimensional jet with side walls have been studied experimentally. Three kinds of cylindrical walls and a flat wall were provided as the side walls, and they were combined and attached to a nozzle. Nine types of side wall conditions were investigated. Velocity was measured by a hot-wire probe and the separation point was measured by a Pitot tube. Mean velocity profiles, the growth of the jet half-width, the decay of jet maximum velocity, and the attachment distance were clarified. When cylindrical walls with different radii are installed, the flow pattern changes markedly depending on the velocity of the jet. A striking increase in the jet half-width is related to the separation of flow from the smaller cylindrical wall just behind the nozzle.

Key Words: Fluid Mechanics, Cylindrical Wall Jet, Coanda Effect, Turbulence, Separation, Velocity Distribution

1. Introduction

A two-dimensional turbulent jet along a wall and a curved wall (in this paper, referred to as a plane wall jet) is important and useful industrially because such a flow can be seen at the nozzles of air-conditioners and air-curtains. Moreover, wall jets are used to delay boundary-layer separation, to either enhance or suppress convective heat transfer between a surface and the fluid surrounding it and to construct a new type of air classifier which separates fine particles. Therefore, many reports have appeared about the plane wall jet and the effects of streamwise curvature on the velocity and fluctuating velocity distribution have been studied⁽¹⁾⁻⁽¹³⁾. The effect of a nozzle width on the flow characteristics was investigated by Shakouchi and Onohara⁽¹⁰⁾ and a comparison was made between a cylindrical wall jet and its plane equivalent by Neuendorf and Wagnanski⁽¹²⁾. However, most of papers deal with the case of a side wall only on one side and the effect of a boundary condition at the nozzle exit on the flow is still unknown. It is worth examining the flow characteristics of a plane wall jet with side walls that have different curvatures on both sides, because such a flow may be appeared

at the nozzle of air-conditioner. From a viewpoint of the flow stability, when a plane wall jet flows along a convex wall, the streamline has a curvature, so that the flow near the wall becomes stable and the flow outside becomes unstable. Therefore, it is also interesting to clarify the effect of the presence of both walls on the flow stability.

In this study, the flow characteristics of a plane wall jet with side walls on both sides have been evaluated experimentally. The effect of the presence of both walls on the velocity profile, the jet half-width, the decay of the velocity, and the attachment distance are clarified, and novel flow patterns of the plane wall jet are shown.

Nomenclature

a : nozzle height (= 10 mm)
 b_y : jet half-width
 R_L, R_M, R_S : radii of cylindrical walls
 U : mean velocity
 U_o : mean velocity at nozzle exit
 U_m : maximum velocity of jet profile
 x, y : co-ordinates along and perpendicular to jet ($x=0$ at nozzle, $y=0$ on wall) (see Fig. 1)
 x_a : attachment distance

2. Experimental Apparatus and Procedure

Figure 1 shows the setup of the side walls and the coordinate system. Three kinds of cylindrical walls (L, M, and S) and a flat wall can be attached to the nozzle smoothly, and nine types of side wall conditions are in-

* Received 15th February, 2006 (No. 06-4035)

** Faculty of Engineering, Gifu University, 1-1 Yanagido, Gifu-shi, Gifu 501-1193, Japan.
 E-mail: imao@gifu-u.ac.jp

*** Kani Technical High School, 2358-1 Nakaedo, Kani, Gifu 509-0202, Japan

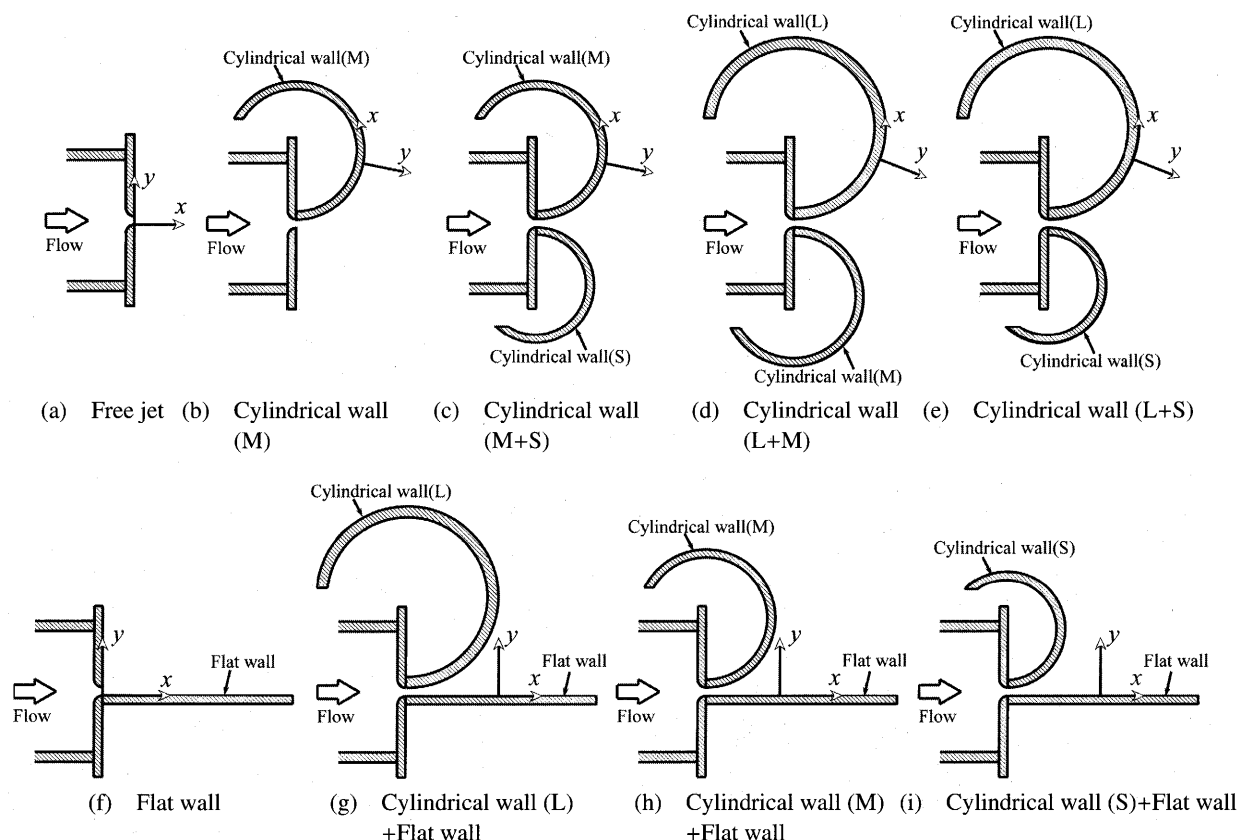


Fig. 1 Experimental apparatus

investigated here, including the case of cylindrical walls of the same radius (M+M, not shown in Fig. 1). The radii of the cylindrical walls are $R_L = 108$ mm, $R_M = 82.5$ mm, and $R_S = 70$ mm. As shown in the following, the jet flows along the larger cylindrical wall, so that the x -axis is chosen on the larger cylindrical wall or the flat wall and y -axis is chosen perpendicular to the wall. The nozzle is rectangular, and its dimensions are $200 \text{ mm} \times 10 \text{ mm}$ and its aspect ratio is 20. The corner of the nozzle is rounded to a quarter circle of $r = 10$ mm. To maintain the two-dimensionality of the flow, two large boards are installed at both ends of the nozzle. The uniformity of the flow in the transverse direction, i.e. two-dimensionality, was confirmed by the measurement of mean velocity profiles at several cross sections in the transverse direction. Measured separation points were much the same in the transverse direction, which also showed two-dimensionality of the flow. Accordingly, the velocity profiles along the center line are shown in the following. Mean velocity profiles were measured by a hot-wire probe. Tungsten filament of 5 micrometer in diameter and 1 mm in active length was used as hot-wire sensor. The I-type probe was used here and the probe was inserted into the flow from the downstream position by a support without disturbing the flow. The fluctuating velocity signals were stored in a personal computer with 10 kHz sampling rate through 5 kHz low-pass filters and the time averaged value were taken over

26 seconds. The separation point was determined by the pressure measurement using a boundary layer Pitot tube, which thickness was 0.5 mm. Flow patterns were visualized by smoke, which was generated by a stage-smoke device and injected into the blower, and the flow patterns were recorded as a movie with a digital video camera. The measurements of the velocity profile and the separation point were carried out under $U_o = 10 \sim 30 \text{ m/s}$. The Reynolds number based on the nozzle height $a (= 10 \text{ mm})$ is $(0.66 \sim 2.0) \times 10^4$.

3. Results and Discussion

At first, a free jet, i.e., without side walls, was examined. Figure 2 shows the mean velocity profiles of the free jet in the downstream section. In this figure, the velocity was normalized by the mean velocity at nozzle exit U_o . In the developed region of the free jet, the similarity of the velocity profile was confirmed, and the jet half-width grew linearly (proportional to x), and the maximum velocity decreased in proportion to $x^{-0.5}$ (not shown). These facts are in good agreement with Ref. (14) for any jet velocity.

3.1 Wall jet with two cylindrical walls

Mean velocity profiles for $U_o = 10 \text{ m/s}$ when two cylindrical walls are installed are shown in Fig. 3. In this figure and in the following, R denotes the radius of the larger cylindrical wall because the jet flows along the larger one. The values $x/R = 0.79, 1.57, \text{ and } 2.36$ corre-

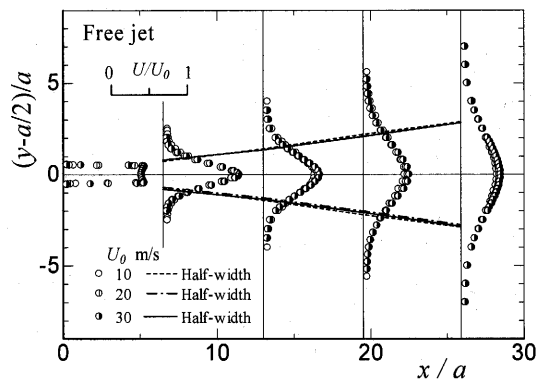
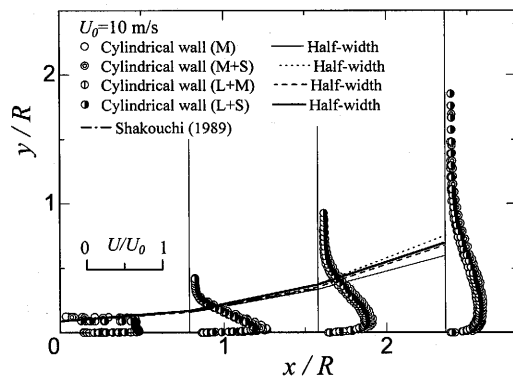
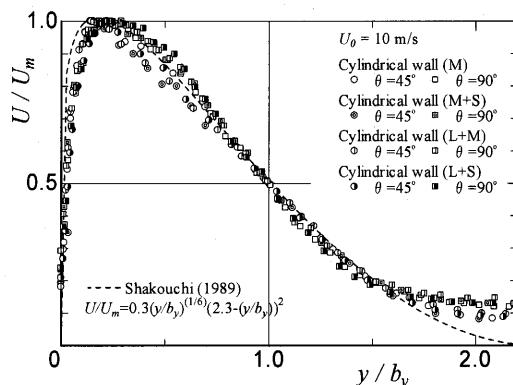
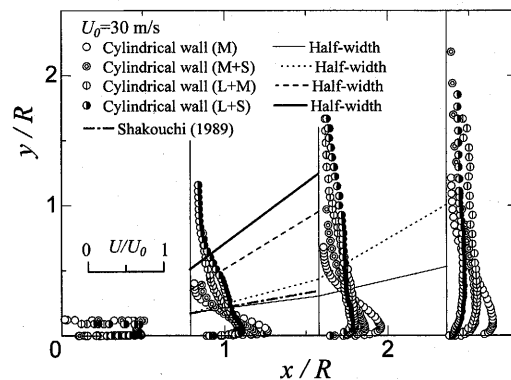
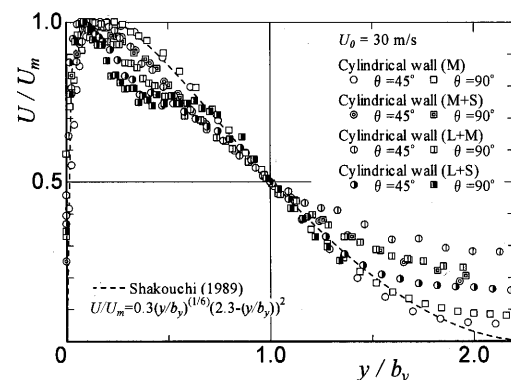


Fig. 2 Mean velocity profile and jet half-width of free jet

Fig. 3 Mean velocity profile and jet half-width of cylindrical wall jet ($U_0 = 10$ m/s)Fig. 4 Mean velocity profile of cylindrical wall jet ($U_0 = 10$ m/s)

spond to the positions $\theta = 45^\circ$, 90° , and 135° on the larger cylindrical wall, respectively. Here θ is the angle from the nozzle exit. At each section, the similarity of velocity profiles can be seen, and the value of the jet half-width b_y are almost the same and agree with those obtained by Shakouchi et al.⁽⁹⁾ In the case of a cylindrical wall jet, the jet half-width increases more than in the case of the wall jet because of centrifugal force. Comparisons of velocity profiles at each section are shown in Fig. 4. Here, mean velocity U and distance y are normalized by the maximum velocity U_m and the jet half-width b_y , respectively. All

Fig. 5 Mean velocity profile and jet half-width of cylindrical wall jet ($U_0 = 30$ m/s)Fig. 6 Mean velocity profile of cylindrical wall jet ($U_0 = 30$ m/s)

data agree with the velocity distribution shown by the dotted line in the figure, which was obtained analytically by Shakouchi et al.⁽⁹⁾ Therefore, the presence of the smaller cylindrical wall has little effect on the velocity profile in this case. The results obtained for $U_0 = 20$ m/s are about the same as that for $U_0 = 10$ m/s.

Mean velocity profiles for $U_0 = 30$ m/s are shown in Fig. 5. When only one cylindrical wall was installed, both the velocity profile and the jet half-width agreed with those of Shakouchi et al.⁽⁹⁾ However, when two cylindrical walls were installed, the jet spreads quickly in the upstream section, and the jet half-width became more than twice that when one cylindrical wall was installed. The magnitude of the jet half-width seemed to depend on the combination of cylindrical walls. The radius ratios of the cylindrical walls are $R_L/R_S = 1.54$, $R_L/R_M = 1.31$, and $R_M/R_S = 1.18$. The jet half-width increases with an increase in the radius ratio in this case. In the downstream section, there was a case in which the jet half-width could not be determined because the velocity became too small. Velocity profiles nondimensionalized by U_m and b_y are shown in Fig. 6. Unlike the case for $U_0 = 10$ m/s (Fig. 4), the profiles are not similar, and the velocity in the outer region ($y > b_y$) became large whereas that in the inner region ($y < b_y$) became a zigzag type. The latter may be attributed

to flow separation. The reason for the considerable change in the flow characteristics is discussed later.

When two cylindrical walls with same dimension were installed, the jet became very unstable. The jet sometimes flowed without adhering to either cylindrical wall, whereas sometimes it adhered to one of the cylindrical walls. In this case, the flow was very sensitive to disturbances such as the insertion of a probe, which meant that velocity measurement could not be carried out, although an unstable flow situation could be identified by flow visualization.

3.2 Wall jet with flat wall and cylindrical wall

Figure 7 shows the mean velocity profiles for $U_0 = 10$ m/s when a flat wall and a cylindrical wall were installed. The jet flowed along the flat wall in this case. Profiles were almost the same at each section, and the jet half-width increased proportionally to $x^{(14)}$. There was a tendency for the jet half-width to increase slowly with an increase in the radius of the cylindrical wall.

Velocity profiles for $U_0 = 30$ m/s are shown in Fig. 8. The increase in U_0 results in an increase in the jet half-width, and in some cases the jet half-width increases to near the twice that of the wall jet. The increasing rate of the jet half-width in this case is almost linear and different

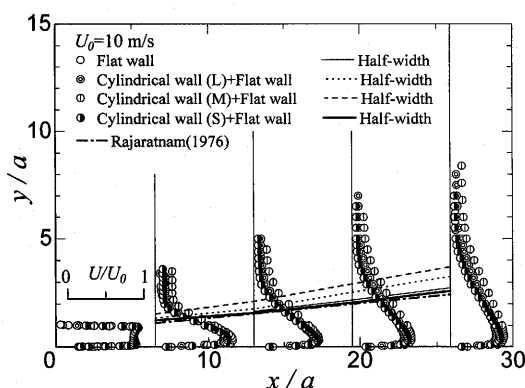


Fig. 7 Mean velocity profile and jet half-width of wall jet with cylindrical wall ($U_0 = 10$ m/s)

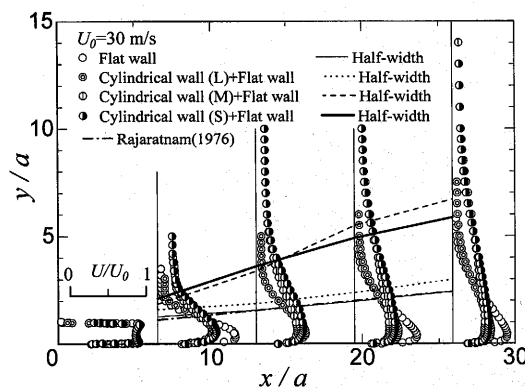


Fig. 8 Mean velocity profile and jet half-width of wall jet with cylindrical wall ($U_0 = 30$ m/s)

from the case in Fig. 5. In this configuration, the nozzle exit is regarded as a diffuser, and it is expected that the separation point on the cylindrical wall near the nozzle exit influences the flow significantly. Velocity profiles nondimensionalized by U_m and b_y are shown in Fig. 9. The dotted line in this figure shows the empirical formula for the wall jet obtained by Verhoff⁽¹⁵⁾. Profiles are similar in the inner region ($y < b_y$) because there is no separation.

3.3 Maximum velocity and attachment distance

Figure 10 shows the decay of the maximum velocity U_m/U_0 when cylindrical walls were installed. In the case of a cylindrical wall jet, the maximum velocity decays in proportion to $x^{-0.5}$ in the developed region, the same as for the free jet and the wall jet. Then it decays in proportion to $x^{-1.8}$ in the downstream region⁽⁹⁾. Qualitative agreement of its decay can be seen, but the maximum velocity starts to decay in proportion to $x^{-1.8}$ at smaller values of x , even when one cylindrical wall is installed. This may arise because the ratio of the cylinder radius to the nozzle height is $10.8 \sim 7.0$ in this experiment, whereas its value is 20 in Ref. (9). Moreover, when two cylindrical walls are installed, the maximum velocity decreases more for smaller values of x , and the core region becomes very

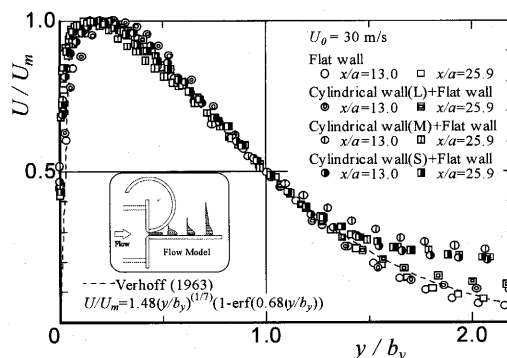


Fig. 9 Mean velocity profile of wall jet with cylindrical wall ($U_0 = 30$ m/s)

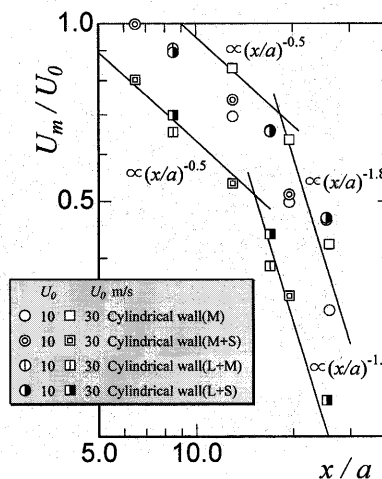


Fig. 10 Decay of maximum velocity (cylindrical wall jet)

short. The decay of the maximum velocity when a flat wall and a cylindrical wall are installed is shown in Fig. 11. The existence of the cylindrical wall causes marked decay of the maximum velocity in the upstream region, where the maximum velocity decreases in proportion to $x^{-0.5}$.

Figure 12 shows the attachment distance x_a , which is

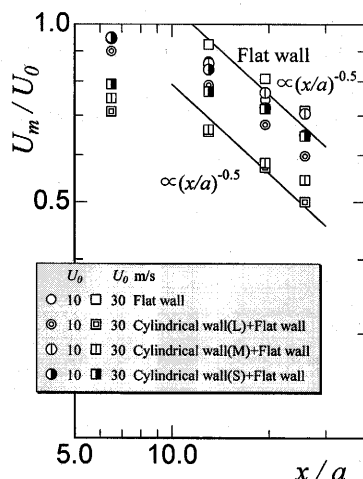


Fig. 11 Decay of maximum velocity (wall jet with cylindrical wall)

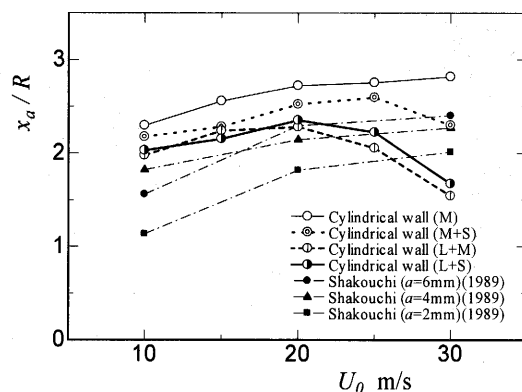


Fig. 12 Attachment distance of cylindrical wall jet

the distance from the nozzle exit to the separation point determined by the Pitot tube. When the Pitot tube is moved along the cylindrical surface in the x -direction, the sign of the pressure changes at the separation point. From a comparison between the measured separation point and the result of the flow visualization by oil-film method, quantitative agreement was obtained between them. The attachment distance x_a is also normalized by the radius of the larger cylindrical wall, and the values $x_a/R = 0.79, 1.57$, and 2.36 correspond to the positions $\theta = 45^\circ, 90^\circ$, and 135° on the larger cylindrical wall, respectively. For the cylindrical wall jet, the attachment distance increases with an increase in the jet velocity⁽¹⁰⁾. When two cylindrical walls are installed, the attachment distance shows a local maximum value and then decreases with an increase in the jet velocity. Therefore, with increasing jet velocity, the jet width is enlarged, the maximum velocity decays markedly, and the separation point moves to an upstream position when two cylindrical walls are present.

The strong dependence of the flow characteristics on the exit velocity U_0 is considered as follows. When a plane wall jet flows along a cylindrical wall, the flow is regarded as a kind of the flow between concentric cylinders with the outer rotating cylinder. This flow is stable for small disturbances and the critical Reynolds number is rather large. According to the experiment by Yamada and Watanabe⁽¹⁶⁾, the critical Reynolds number for our apparatus corresponds to $8000 \sim 12000$. Here, the Reynolds number is converted to that defined in this paper. In this experiment, the exit velocity $U_0 = 10, 20, 30$ m/s corresponds to $Re = 6600, 13200, 20000$, respectively. Although the flow situation is not exactly the same between this flow and the flow between rotating cylinders, it is considered that the flow instability affects this plane wall jet when the Reynolds number exceeds a critical value. There is also strong dependence on the radius ratio of the cylindrical walls. The plane wall jet becomes unstable with an

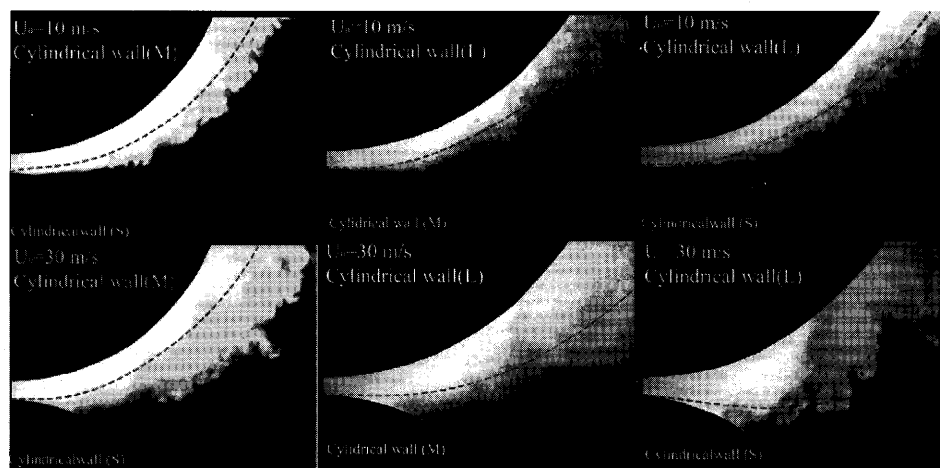


Fig. 13 Visualized flow pattern of cylindrical wall jet

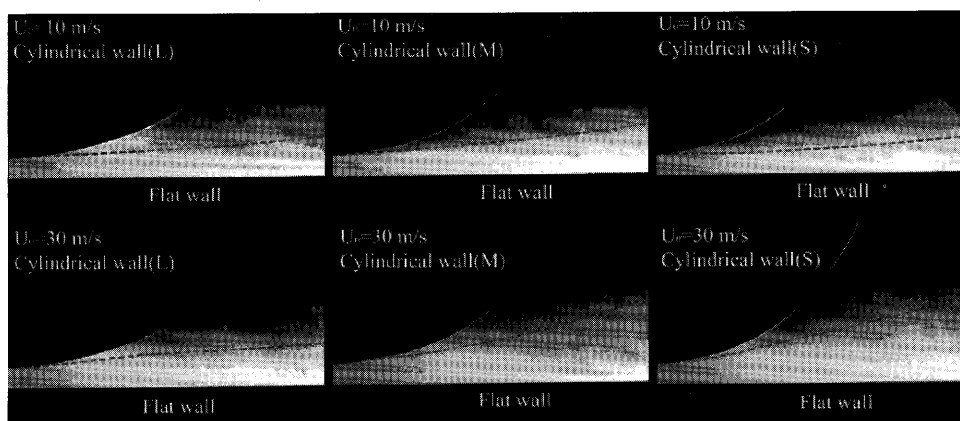


Fig. 14 Visualized flow pattern of wall jet with cylindrical wall

increase in the radius ratio in this study, but the cylindrical walls used here are only three kinds and the combination is limited. An exhaustive study may be necessary to clarify the dependence on the radius ratio in detail.

3.4 Flow visualization

Figure 13 shows the visualized flow patterns when two cylindrical walls are installed. The dotted line shows the position of the jet half-width obtained from the velocity measurement. The flow seemed to be steady at $U_0 = 10$ m/s and an almost constant flow pattern was obtained. However, the flow became unsteady at $U_0 = 30$ m/s, and the flow pattern varied continuously. It was confirmed from the observation of the movie that the separation point on the smaller cylindrical wall varied considerably, and consequently the extent of the smoke also varied greatly. These facts show that the wall jet with two cylindrical walls becomes unsteady with an increase in jet velocity.

Figure 14 shows the flow patterns when a flat wall and a cylindrical wall were installed. In this case, the jet flow was steady compared to the former case. Flow patterns did not vary markedly even at $U_0 = 30$ m/s, and the extent of the smoke was proportional to the jet half-width.

4. Conclusions

An experimental study was carried out on the flow characteristics of a plane wall jet with side walls. The results are summarized as follows.

- (1) When cylindrical walls with different radii are installed, the jet attaches to the larger cylindrical wall, and if a flat wall is installed, the jet flows along it.
- (2) When cylindrical walls with different radii are installed, the jet half-width increases markedly with an increase in the jet velocity, and its width becomes more than twice that when a cylindrical wall is installed. The maximum velocity decays greatly.
- (3) In the case described in (2), the attachment distance, which is the distance from the nozzle exit to the separation point, decreases as jet velocity increases.
- (4) Flow visualization revealed that the significant

increase in jet width is related to the flow separation from the smaller cylindrical wall just behind the nozzle.

References

- (1) Sridhar, K. and Tu, P.K.C., Experimental Investigation of Curvature Effects on Turbulent Wall Jets, *Aeronaut. J. Royal Aeronaut. Soc.*, Vol.73 (1969), pp.977–981.
- (2) Manian, V.S., McDonald, T.W. and Besant, R.W., Heat Transfer Measurements in Cylindrical Wall Jets, *Int. J. Heat and Mass Transfer*, Vol.12, No.6 (1969), pp.673–679.
- (3) Patanker, U.M. and Sridhar, K., Three-Dimensional Curved Wall Jets, *Trans. ASME, J. Basic Engng.*, (1972), pp.339–344.
- (4) Miyazaki, H. and Sparrow, E.M., Flow and Heat Transfer in Curved Wall Jets on Circular Surfaces, *Int. J. Heat and Mass Transfer*, Vol.18, No.12 (1975), pp.1351–1360.
- (5) Wilson, D.J. and Goldstein, R.J., Turbulent Wall Jets with Cylindrical Streamwise Surface Curvature, *Trans. ASME I, J. Fluids Engng.*, Vol.98 (1976), pp.550–557.
- (6) Guitton, D.E. and Newmann, B.G., Self-Preserving Turbulent Wall Jets over Convex Surfaces, *J. Fluid Mech.*, Vol.81, No.1 (1977), pp.155–185.
- (7) Kobayashi, R. and Fujisawa, N., Curvature Effects on Two-Dimensional Turbulent Wall Jets, *Ing. Arch.*, Vol.53 (1983), pp.409–417.
- (8) Fujisawa, N. and Kobayashi, R., Turbulence Characteristics of Wall Jets along Strong Convex Surfaces, *J. Mech. Sci.*, Vol.29 (1987), pp.311–320.
- (9) Shakouchi, T., Onohara, Y. and Kato, S., Analysis of a Two-Dimensional, Turbulent Wall Jet along a Circular Cylinder (Velocity and Pressure Distributions), *JSME Int. J., Ser. II*, Vol.32, No.3 (1989), pp.332–339.
- (10) Shakouchi, T. and Onohara, Y., Analysis of a Two-Dimensional, Turbulent Wall Jet along a Circular Cylinder (Effects of Nozzle Width), *Trans. Jpn. Soc. Mech. Eng.*, (in Japanese), Vol.55, No.511, B (1989), pp.662–669.
- (11) Shakouchi, T., Onohara, Y. and Kato, S., Analysis of a Two-Dimensional, Turbulent Wall Jet along a Circular Cylinder (Effects of Nozzle Exit Velocity Profile and Injection Angle), *Trans. Jpn. Soc. Mech. Eng.*, (in

- Japanese), Vol.56, No.532, B (1990), pp.3650–3657.
 - (12) Neuendorf, R. and Wagnanski, I., On a Turbulent Wall Jet Flowing over a Circular Cylinder, *J. Fluid Mech.*, Vol.381 (1999), pp.1–25.
 - (13) Shakouchi, T., *Jet Flow Engineering (Fundamentals and Application)*, (in Japanese), (2004), Morikita Shuppan, Tokyo.
 - (14) Rajaratnam, N., *Turbulent Jets*, (1976), Elsevier Scientific Publishing Company, Amsterdam.
 - (15) Verhoff, A., *The Two-Dimensional Turbulent Wall Jet with and without an External Stream*, Rep.626, Princeton Univ., (1963).
 - (16) Yamada, Y. and Watanabe, S., Frictional Moment and Pressure Drop of the Flow through Co-Axial Cylinders with an Outer Rotating Cylinder, *Bulletin JSME*, Vol.16, No.93 (1973), pp.551–559.
-